Neutron capture in the r-process

Rebecca Surman[∗]

Department of Physics and Astronomy, Union College, Schenectady, New York 12308, USA
E-mail: surmanr@union.edu

G.C. McLaughlin

Department of Physics, North Carolina State University, Raleigh, North Carolina 27695, USA

M. Mumpower

Department of Physics, North Carolina State University, Raleigh, North Carolina 27695, USA

W.R. Hix

Physics Division, Oak Ridge National Laboratory, Oak Ridge, Tennessee, 37831, USA

K. Jones

Department of Physics, University of Tennessee, Knoxville, Tennessee, USA

Recently we have shown that neutron capture rates on nuclei near stability significantly influence the *r*-process abundance pattern. We discuss the different mechanisms by which the abundance pattern is sensitive to the capture rates and identify key nuclei whose rates are of particular importance. Here we consider nuclei in the $A = 130$ and $A = 80$ regions.

[∗]Speaker.

1. Introduction

The formation of about half of the solar system heavy element abundancess has long been attributed to rapid neutron capture, or *r*-process, nucleosynthesis [1, 2]. However, much remains to be learned about this process, both in the astrophysics of the environment(s) in which it occurs and in the nuclear physics of the thousands of unstable nuclei produced. Here we focus on the latter.

It has traditionally been assumed that nuclear masses and beta-decay rates are the most important pieces of nuclear data for the *r* process. In the classic picture of the *r*-process (see, e.g., [3]), neutron captures on seed nuclei proceed in conditions of high temperature and free neutron density, such that equilibrium obtains between neutron captures and photodissociations. While this (n,γ)-(γ,n) equilibrium persists, the nuclear abundances along an isotopic chain are determined by the neutron separation energies, via the Saha equation. The nuclear masses are therefore key in shaping the *r*-process abundance pattern. The isotopic chains are linked by beta decays; beta-decay rates therefore determine not only the relative abundances of the isotopic chains but also the overall timescale for the *r*-process to proceed from iron-peak seeds to the $A = 195$ peak.

In contrast, the importance of neutron capture rates has only recently begun to be recognized. In the traditional view, the *r*-process abundance pattern is largely set by time (n,γ)-(γ,n) equilibrium begins to freeze out, and so individual values of the neutron capture rates are thought to have limited impact. However a number of groups [4, 5, 6, 7] have investigated simultaneous modifications of all capture rates, and it has been found that this can alter the time until freezeout. In addition, modern dynamical nuclear network calculations demonstrate that important changes in the *r*-process abundance pattern take place as material falls out of (n,γ)-(γ,n) equilibrium, e.g., [8], and in some cases, such as in a cold *r*-process [9], (n,γ)-(γ,n) equilibrium may never even be established. In [10], we introduce the basic theory behind how individual neutron capture rates can influence the global *r*-process abundance pattern during freezeout from (n,γ)-(γ,n) equilibrium. While in [10] we focused on neutron capture in the $A = 130$ region, the mechanisms by which the influence occurs are more general and apply to nuclei in all three peak regions. Here we review the two basic mechanisms, and we show that they operate in the same way in the $A = 80$ region.

2. Neutron capture effects during freezeout

In [11, 10], we identify two basic mechanisms by which an individual neutron capture rate can influence the global *r*-process abundance pattern, for an *r*-process that freezes out from (n,γ)-(γ,n) equilibrium. The first, a photodissociation effect, operates at the onset of freezeout, while most (populated) nuclei are still in equilibrium but material has begun to shift from the very neutron-rich back toward stability. The second, a neutron capture effect, happens later in freezeout, during the capture of the final remaining free neutrons.

To illustrate the photodissociation effect, we consider the example of ^{131}Cd in a baseline supernova neutrino-driven wind simulation characterized by entropy $s/k = 100$, timescale 0.1 s, and $Y_e = 0.26$. Just before freezeout the most populated nuclei in the simulation are at the top of the $N = 82$ closed shell region, ^{129}Ag, ^{132}Cd, and ^{133}In, as depicted in Fig. 1. As the free neutrons are used up, equilibrium favors less neutron-rich isotopes, and material begins to shift toward stability. If the temperature is still fairly high ($\sim 10^9$ K) while the neutrons are depleted, as in this
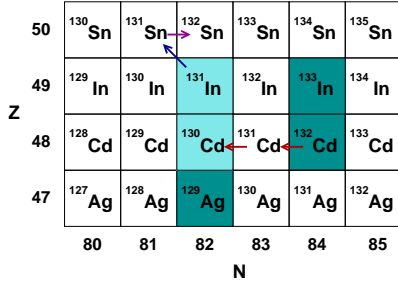
Figure 1: Shows the nuclear flow in the region of ^{131}Cd and ^{131}Sn for the baseline simulation. The dark shaded squares show the isotopes of maximum abundance for each element at the beginning of freezeout from (n,γ)-(γ,n) equilibrium, and the lighter shaded squares show the most populated isotopes at a somewhat later time. Red arrows indicate photodissociation, the purple arrow indicates neutron capture, and the blue arrow shows beta decay [10].

simulation, the shift to stability will begin with photodissociation to less neutron-rich isotopes. Nuclei with slower-than-average photodissociation rates, therefore, will be 'stuck', particularly if the beta-decay lifetime is also long. This is the case with ^{132}Cd in our baseline simulation. We then run a second simulation, in which the neutron capture rate of ^{131}Cd is increased by a factor of 10. This acts also to increase the photodissociation rate of ^{132}Cd by the same factor, as the two are related by detailed balance. In the second simulation, material is no longer trapped at ^{132}Cd as equilibrium fails; it photodissociates to ^{131}Cd and then to ^{130}Cd, as depicted in Fig. 1. Since ^{132}Cd is so abundant, this releases many neutrons that are then available for capture elsewhere. The left panel of Fig. 2 shows the rate of neutron captures relative to the baseline simulation for the $A = 130$ peak region and the region above the $A = 130$ peak. The increased rate of ^{132}Cd photodissociations compared to the baseline simulation causes a sharp decrease in the captures in the $A = 130$ peak region and a corresponding increase in the number of captures elsewhere.
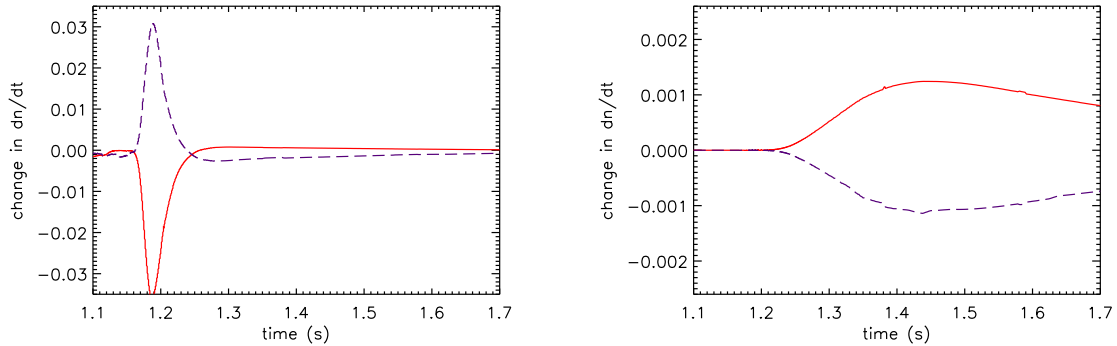

Figure 2: Shows the rate of neutron capture within (solid red line) and above (purple dashed line) the $A = 130$ region relative to the baseline simulation, for simulations in which a single neutron capture rate is increased—that of ^{131}Cd by a factor of 10 (left panel, photodissociation effect) or of ^{131}Sn by a factor of 100 (right panel, neutron capture effect) [10].

At later times in the same baseline simulation, the temperature drops, and material moves back toward stability primarily via beta decay. However, neutron capture has not entirely ceased, as the free neutron abundance is replentished slightly at late times by beta-delayed neutron emission. Abundant nuclei with high neutron capture rates can drain these last available neutrons. For example, at late times ^{131}Sn becomes highly populated as it is a beta-decay product of the closed-shell nucleus ^{131}In, as depicted in Fig. 1. A simulation where the neutron capture rate of ^{131}Sn

is increased by a factor of 100 shows a significant increase in the rate of neutron capture in the $A = 130$ peak region compared to the baseline simulation, with a corresponding decrease in the neutron captures elsewhere, as shown in the right panel of Fig. 2.

3. Influential neutron capture rates

In [10] we identified a subset of nuclei in the $A = 130$ region whose capture rates have significant leverage on the global *r*-process abundance pattern, for a range of wind parameters and nuclear data sets. These nuclei are shown in Fig. 3.
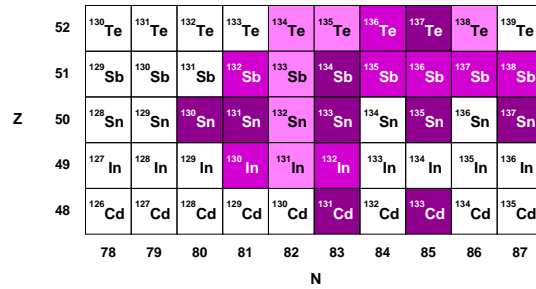

Figure 3: Shows the nuclei that have neutron capture rates which effect a $\sim 5\%$ or more abundance change for a rate increase or decrease of a factor of 10 (dark colored squares), a factor of 50 (medium color squares), and a factor of 100 to 1000 (light color squares) [10].

4. $A = 80$ **region**

We have recently begun similar neutron capture sensitivity studies for the $A = 80$ region. While the wind conditions required to reproduce the solar abundance pattern in this region are quite different, our preliminary studies show the same neutron capture mechanism operates here as well, as shown, for example, in Fig. 4. These studies also suggest that the larger sensitivity to odd-*N* capture rates to the left of the closed shell region, as seen in the $A = 130$ [10] and $A = 195$ [8] cases, is also found in the $A = 80$ region.
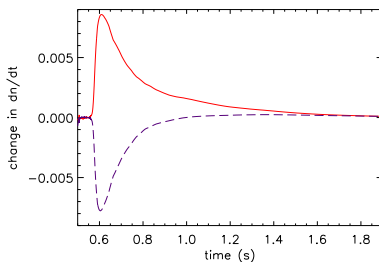

Figure 4: Shows the effect of increasing the neutron capture rate of ^{78}Cu by a factor of 100 relative to a baseline simulation taken from [12]. The solid red line shows the rate of neutrons captured in the $A = 80$ peak region relative to the baseline simulation and the dashed purple line shows the rate of neutrons captured above the $A = 80$ region. This is an example of the neutron capture effect, similar to the right panel of Fig. 2.

5. Conclusion

The *r*-process abundance pattern is shaped by nuclear physics. While beta decay rates and nuclear masses may have the greatest leverage on this pattern, we have shown neutron capture

rates also play an important role in finalizing the abundance distribution. We have described two mechanisms by which individual neutron capture rates can impact the global *r*-process abundance pattern—an early time photodissociation effect and a late time neutron capture effect—and we have identified a set of influential rates in the $A = 130$ region. We look forward to future theoretical and experimental efforts to improve cross section values and further clarify these effects.

Acknowledgments

References

[1] E. M. Burbidge, G. R. Burbidge, W. A. Fowler, and F. Hoyle. Synthesis of the Elements in Stars. *Reviews of Modern Physics*, 29:547–650, 1957.

[2] A. G. W. Cameron. *Chalk River Rep.*, CRL-41, 1957.

[3] J. J. Cowan, F.-K. Thielemann, and J. W. Truran. Nuclear chronometers from the r-process and the age of the galaxy. *Astrophysical Journal*, 323:543–552, December 1987.

[4] S. Goriely. Radiative neutron captures by neutron-rich nuclei and the r-process nucleosynthesis. *Physics Letters B*, 436:10–18, September 1998.

[5] T. Rauscher. Neutron Captures and the r-Process. In Y.-Z. Qian, E. Rehm, and H. Schatz, editors, *The r-Process: The Astrophysical Origin of the Heavy Elements and Related Rare Isotope Accelerator Physics*, pages 63–+, 2004.

[6] T. Rauscher. Neutron capture in the r-process – do we know them and does it make any difference? *Nuclear Physics A*, 758:655, 2005.

[7] K. Farouqi, K.-L. Kratz, B. Pfeiffer, T. Rauscher, and F.-K. Thielemann. Neutron captures and the r-process. In A. Woehr and A. Aprahamian, editors, *Capture Gamma-Ray Spectroscopy and Related Topics*, volume 819 of *American Institute of Physics Conference Series*, pages 419–422, March 2006.

[8] R. Surman and J. Engel. Changes in r-process abundances at late times. *Physical Review C*, 64(3):035801–+, September 2001.

[9] S. Wanajo. Cold r-Process in Neutrino-driven Winds. *The Astrophysical Journal*, 666:L77–L80, September 2007.

[10] R. Surman, J. Beun, G. C. McLaughlin, and W. R. Hix. Neutron capture rates near A=130 that effect a global change to the r-process abundance distribution. *Physical Review C*, 79(4):045809–+, April 2009.

[11] J. Beun, J. C. Blackmon, W. R. Hix, G. C. McLaughlin, M. S. Smith, and R. Surman. Neutron capture on Sn-130 during r-process freeze-out. *Journal of Physics G Nuclear Physics*, 36(2):025201–+, February 2009.

[12] R. Surman, G. C. McLaughlin, M. Ruffert, H.-T. Janka, and W. R. Hix. r-Process Nucleosynthesis in Hot Accretion Disk Flows from Black Hole-Neutron Star Mergers. *The Astrophysical Journal*, 679:L117–L120, June 2008.